



Uncertainty analysis for the assembly and core simulation of BEAVRS at the HZP conditions



Chenghui Wan^a, Liangzhi Cao^{a,*}, Hongchun Wu^a, Wei Shen^{a,b}

^a School of Nuclear Science and Technology, Xi'an Jiaotong University, Xi'an 710049, China

^b Canadian Nuclear Safety Commission, Ottawa, Ontario, Canada

HIGHLIGHTS

- Uncertainty analysis has been completed based on the “two-step” scheme.
- Uncertainty analysis has been performed to BEAVRS at HZP.
- For lattice calculations, the few-group constant's uncertainty was quantified.
- For core simulation, uncertainties of k_{eff} and power distributions were quantified.

ARTICLE INFO

Article history:

Received 25 September 2016

Received in revised form 9 February 2017

Accepted 14 February 2017

Keywords:

Uncertainty analysis
Lattice calculation
Core simulation
BEAVRS

ABSTRACT

Based on the “two-step” scheme for the reactor-physics calculations, the capability of uncertainty analysis for the core simulations has been implemented in the UNICORN code, an in-house code for the sensitivity and uncertainty analysis of the reactor-physics calculations. Applying the statistical sampling method, the nuclear-data uncertainties can be propagated to the important predictions of the core simulations. The uncertainties of the few-group constants introduced by the uncertainties of the multigroup microscopic cross sections are quantified first for the lattice calculations; the uncertainties of the few-group constants are then propagated to the core multiplication factor and core power distributions for the core simulations. Up to now, our in-house lattice code NECP-CACTI and the neutron-diffusion solver NECP-VIOLET have been implemented in UNICORN for the steady-state core simulations based on the “two-step” scheme. With NECP-CACTI and NECP-VIOLET, the modeling and simulation of the steady-state BEAVRS benchmark problem at the HZP conditions was performed, and the results were compared with those obtained by CASMO-4E. Based on the modeling and simulation, the UNICORN code has been applied to perform the uncertainty analysis for BEAVRS at HZP. The uncertainty results of the eigenvalues and two-group constants for the lattice calculations and the multiplication factor and the power distributions for the steady-state core simulations are obtained and analyzed in detail.

© 2017 Elsevier B.V. All rights reserved.

1. Introduction

With the increasing demands for the reactor design and safety analysis to be provided with their confidence bounds, the requirements of uncertainty evaluations for the best-estimate calculations of reactor has been proposed. To satisfy the requirements, the UAM (“Uncertainty Analysis in Modeling”) expert group has been organized by the OECD/NEA to establish the benchmarks for the uncertainty analysis in the best-estimate modeling of the coupled multi-physics and multi-scale LWR system (Ivanov et al., 2013).

According to the UAM benchmarks, uncertainties in the LWR system calculations at all stages should be determined and quantified. As the reactor-physics calculations are prerequisite for the predictions of the reactor system, and the uncertainties introduced by the neutronics calculations impact the subsequent calculations and analysis, hence the uncertainty analysis has been firstly focused on the neutronics phase to quantify the uncertainties of the reactor-physics predictions. According to UAM, for the phase of the lattice physics, the objective is focused on quantifying the uncertainties of the few-group constants; for the phase of the core physics, uncertainty quantifications for the important predictions of the core steady-state stand-alone neutronics calculations are focused on. According to the previous researches, the nuclear-data uncertainty has been proved to be one of the most significant

* Corresponding author at: School of Nuclear Science and Technology, Xi'an Jiaotong University, 28 Xianning West Road, Xi'an 710049, China.

E-mail address: caolz@mail.xjtu.edu.cn (L. Cao).

uncertainty sources for the reactor-physics calculations and received the most focus (Wieselquist et al., 2012; Yankov et al., 2012; Foad and Takeda, 2015). According to the uncertainty-analysis scheme for the reactor-physics calculations proposed by UAM, the nuclear-data uncertainties would be propagated first to the lattice calculations and then to the core simulations.

In order to propagate the nuclear-data uncertainties to the reactor-physics responses, two kinds of methodologies have been proposed and applied widely: the deterministic method and the statistical sampling method. For the deterministic method, the uncertainty analysis is performed using the sandwich formula based on the sensitivity analysis, for which the perturbation theory (PT) (Pusa, 2012) and the direct numerical perturbation (DNP) method (Ball et al., 2013) were widely utilized. Comparing the PT and DNP methods, the PT method need to establish different perturbation models for different responses; while for the DNP method, no extra effort is needed for different responses, but larger calculation cost is required than the PT method. For the statistical sampling (SS) method (Wieselquist et al., 2012), uncertainty analysis is based on the response samples, which are obtained by the reactor-physics calculations with corresponding cross-section samples obtained from the nuclear-data uncertainty ranges. With comparisons of the deterministic method and the statistical sampling method for uncertainty analysis, the PT-based deterministic method has the advantage of high calculation efficiency and the disadvantages of the first-order approximation and of establishing different perturbation models for different responses; the statistical sampling method has the disadvantage of large calculation cost and the obvious advantages of non-linearity and of no limitation or extra efforts for different responses.

Based on the DNP method and SS method, our home-developed UNICORN code has the capability of sensitivity and uncertainty analysis for the lattice calculations in our previous work (Wan et al., 2015; Zu et al., 2016). In this paper, according to the “two-step” scheme for the reactor-physics calculations, the uncertainty-analysis capability of UNICORN has been extended to the steady-state core simulations by application of the SS method. At the phase of the lattice calculations, the uncertainties of the multigroup microscopic cross sections are propagated to the important responses, including the eigenvalues, few-group constants, kinetic parameters and atomic densities with the depletions; then at the phase of the core calculations, the uncertainties of the few-group constants are propagated to the interested responses, including the multiplication factor, power distributions and so on. As both the samples and covariance matrices of the few-group constants can be obtained from the uncertainty analysis of the lattice calculations with the SS method, two corresponding sampling methods can be applied in the uncertainty analysis for the steady-state core simulations: the sampling method based on the relative covariance matrices of the few-group constants and the sampling method based on the samples of the few-group constants. Up to now, DRAGON 5.0 (Marleau et al., 2014) and our home-developed lattice code NECP-CACTI (Li et al., 2015a) are available in UNICORN for the lattice calculations; and our home-developed neutron-diffusion solver NECP-VIOLET (Li et al., 2015b) is available in UNICORN for the steady-state core simulations. With NECP-CACTI and NECP-VIOLET, the modeling and simulation of steady-state BEAVRS benchmark problem (Horelik and Herman, 2013) at the HZP condition was performed. CASMO-4E (Rhodes et al., 2004) was used to verify the modeling and simulation of BEAVRS at HZP with NECP-CACTI and NECP-VIOLET. Based on the modeling and simulation, the UNICORN code has then been applied to perform the uncertainty analysis for BEAVRS at HZP. For the uncertainty analysis to the lattice calculations, the relative uncertainties of the eigenvalues and few-group constants have been quantified; for the uncertainty analysis to

the steady-state core simulation, the relative uncertainties of the multiplication factor and power distributions have been quantified.

This paper is organized as follow. The overview of the UNICORN code is given in Section 2. In Section 3, detailed description of modeling and simulation of the steady-state BEAVRS at HZP has been introduced. Uncertainty analysis for BEAVRS at HZP has been made in Section 4, in which the numerical results and detailed analysis of the uncertainty results are discussed. Summary and conclusions are given in Section 5.

2. Overview of the UNICORN code

In this paper, the uncertainty-analysis capability has been completed in UNICORN according to the “two-step” scheme of the reactor-physics calculations. The flowchart of the UNICORN code is shown in Fig. 1. For the lattice calculations, the sensitivity and uncertainty analysis are performed using the DNP method and SS method respectively. As results of the uncertainty analysis for the lattice calculations applying the SS method, both the samples and covariance matrices of the few-group constants can be obtained and provided to the uncertainty analysis for the core simulations. For uncertainty analysis of the core simulations, two methods based on the samples and covariance matrices of the few-group constants are established and applied in UNICORN respectively. Up to now, the UNICORN code has the capability of performing the uncertainty analysis for the steady-state core simulations using the SS method.

2.1. Uncertainty analysis for the lattice calculations

At the beginning of uncertainty analysis for the lattice calculations, a standard multigroup cross-section format need to be defined by the combined applications of the cross-section information contained in the basic cross-section library and the multigroup microscopic cross-section library with specific format. This standard multigroup cross-section format is designed based on the fact that different lattice codes would utilize different formatted multigroup microscopic cross-section libraries, and with the cross-section information conversion, other lattice codes can be implemented into UNICORN conveniently when needed. In the standard multigroup cross-section format, the integral, basic and resonance cross sections are defined. The integral cross sections include σ_t , σ_s , σ_a and σ_{tr} ; the basic cross sections include $\sigma_{(n,elas)}$, $\sigma_{(n,inel)}$, $\sigma_{(n,2n)}$, $\sigma_{(n,3n)}$, ν , σ_f , σ_γ , $\sigma_{(n,p)}$, $\sigma_{(n,D)}$, $\sigma_{(n,T)}$, $\sigma_{(n,\alpha)}$, $\sigma_{(n,He)}$, $\sigma_{(n,2\alpha)}$ and so on; the resonance cross sections include $\sigma_r t$, $\sigma_r s$, $\sigma_r a$, $\sigma_r f$, $\sigma_r v f$ and $\sigma_r \gamma$. The integral and basic cross sections are defined as the function of the energy groups and temperatures; while the resonance cross sections are defined as function of the energy groups, temperatures and dilution cross sections. Up to now, the cross-section information included in WIMSD-4 (Leszczynski et al., 2007) formatted library for DRAGON5.0 and NECL formatted library (Li et al., 2015a) for NECP-CACTI can be converted to the cross-section information defined in the standard multigroup cross-section format, and vice versa.

Based on the standard multigroup cross-section format, the verified multigroup cross-section perturbation mode (Wan et al., 2015) is applied to perturb the multigroup cross sections to the required values according to the relative perturbation factors, which are generated based on the SS method for uncertainty analysis or the DNP method for sensitivity analysis. After the cross-section perturbations, the multigroup cross-section consistency rules are applied to keep the integral and basic cross sections balance. This step is essential and important, as correct predictions of the lattice calculations can be obtained only by the balanced and

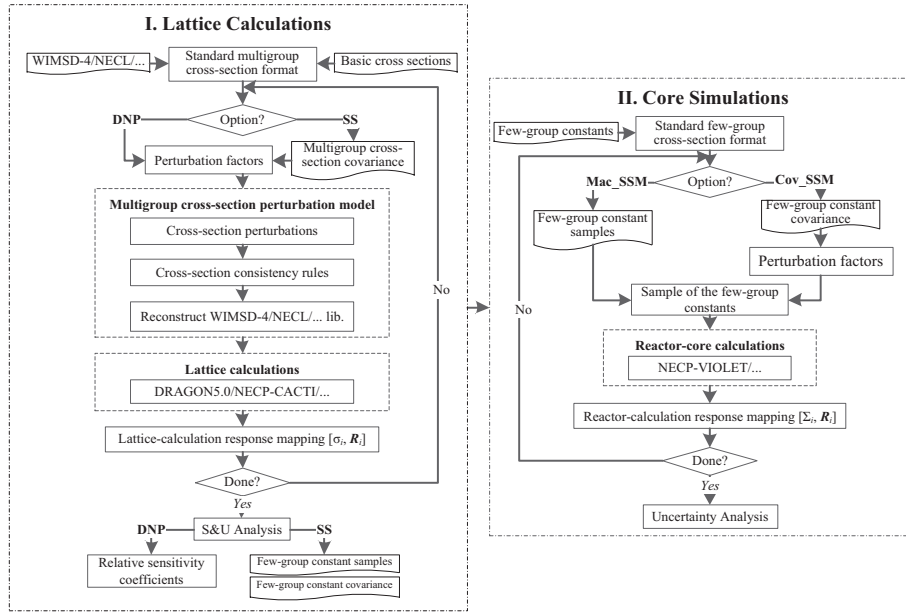


Fig. 1. The flowchart of the UNICORN code.

consistent multigroup cross sections. The perturbed cross-section information contained in the standard multigroup cross-section format are then reconstructed into the perturbed multigroup microscopic cross-section library with specific format, e.g. WIMSD-4 and NECL. Provided with the perturbed multigroup microscopic cross-section library, corresponding lattice code is executed to carry out the lattice calculations.

After the lattice calculations using all of the perturbed multigroup microscopic cross-section libraries, corresponding lattice responses can be obtained. In UNICORN, a standard responses format is also designed, which can cover the important responses of the lattice calculation, including the eigenvalues, few-group constants, kinetic parameters and atomic densities with the depletions. The responses obtained by the executions of DRAGON5.0 and NECP-CACTI can be converted to the standard response format, based on which the sensitivity and uncertainty analysis can be performed. With the SS method for the lattice calculations, not only the covariance matrices of the few-group constants, but also the samples of the few-group constants can be obtained, based on which the uncertainty analysis for the core simulations can be performed.

2.2. Uncertainty analysis for the core simulations

As shown in Fig. 1, at the beginning of uncertainty analysis for the steady-state core simulations, the few-group constants are converted into a standard few-group cross-section format designed and applied in UNICORN. In this format, the few-group constants essential for the steady-state core simulations are defined, including D , Σ_t , Σ_a , $\nu\Sigma_f$, $\kappa\Sigma_f$, Σ_s , χ and $ADFs$ (assembly discontinuity factors). The neutron-diffusion solver NECP-VIOLET is applied to carry out the steady-state core simulations in UNICORN. As the relative covariance matrices and samples of the few-group constants can be obtained in the uncertainty analysis of the lattice calculations with the SS method, there are two corresponding sampling methods can be applied in the uncertainty analysis for the steady-state core simulations: the sampling method based on the relative covariance matrices of the few-group constants and the sampling method based on samples of the few-group constants. In Fig. 1, the option “Cov_SSM” stands for the sampling method applying

the relative covariance matrices of the few-group constants, and the option “Mac_SSM” represents the sampling method applying the samples of the few-group constants. Detailed introductions of these two sampling methods are given in the sub-sections.

For the sampling method applying the relative covariance matrices (“Cov_SSM”), the relative perturbation factors of the few-group constants are generated as shown in Eq. (1).

$$\mathbf{X}_S = \Sigma_r^{1/2} \mathbf{Y}_S + \mathbf{1.0} \quad (1)$$

where the Σ_r represents the relative covariance matrix of the few-group constants; \mathbf{X}_S and \mathbf{Y}_S stand for the samples of the dependent parameters and the independent parameters respectively. Applying Eq. (1), the samples of the relative perturbation factors for the dependent parameters can be easily generated through the samples of the independent parameters. The samples of the relative perturbation factors can be characterized as $\mathbf{X}_S = [x_{1,i}, x_{2,i}, \dots, x_{nX,i}]^T$ ($i = 1, 2, \dots, nS$), in which nX represents the number of the few-group constants and nS stands for the number of samples. With the samples of the relative perturbation factors \mathbf{X}_S and the expectation values of the few-group constants $\boldsymbol{\mu} = [\mu_1, \mu_2, \dots, \mu_{nX}]^T$, the samples for the few-group constants can be generated using Eq. (2).

$$\Sigma_{j,i} = \mu_j x_{j,i} \quad j = 1, 2, \dots, nX; \quad i = 1, 2, \dots, nS \quad (2)$$

where $\Sigma_{j,i}$ represents the i th sample of the j th few-group constants. Moreover, the bootstrap method (Archer et al., 1997) has also been applied to quantify the confidence intervals of the uncertainty results. Detailed introductions of the bootstrap method can be found in our previous work (Wan et al., 2015).

For the sampling method applying the samples of the few-group constants provided by the uncertainty analysis of the lattice calculations (“Mac_SSM”), one sample of the few-group constants is used once a time to carry out the core simulation until all the samples have been used.

The main difference between “Mac_SSM” method and “Cov_SSM” is focused on whether has to re-sample for the few-group constants. As comparison of these two sampling methods: for the “Cov_SSM” method, the samples of the few-group constants should be generated according to corresponding covariance matrices and this will introduce extra statistical errors into the uncertainty results; while the “Mac_SSM” method directly uses the samples

of the few-group constants generated by the uncertainty analysis of the lattice calculations and no extra statistical errors will be introduced into the uncertainty results. Therefore, the “Mac_SSM” method is superior to the “Cov_SSM” method to perform the uncertainty analysis for the core simulations from the view of the calculation scheme. With applying all the samples of the few-group constants, either generated by the relative covariance matrices or direct use of the samples, corresponding samples of the responses of the core simulations can be obtained, based on which the relative uncertainties of the responses can be quantified using the statistical calculations. For the steady-state core simulations, the uncertainties of the multiplication factor and power distributions can be quantified in UNICORN.

3. Core modeling and simulation of BEAVRS

In this section, our home-developed lattice code NECP-CACTI and the neutron-diffusion solver NECP-VIOLET are applied for the steady-state core modeling and simulation of BEAVRS at HZP based on the “two-step” scheme. For the lattice calculations with NECP-CACTI, the two-group constants, with the energy cut-off point for the fast and thermal group set to be 0.625 eV, are generated for the fuel assemblies and the radial baffle reflectors. For the steady-state core simulations with NECP-VIOLET, 2D reactor is simulated without axial buckling. The steady-state core modeling and simulation of BEAVRS at HZP by applications of NECP-CACTI and NECP-VIOLET are compared and verified against the results obtained by CASMO-4E.

3.1. Lattice calculations with NECP-CACTI

The NECP-CACTI (Li et al., 2015a) is our home-developed lattice code, using the subgroup method for the resonance self-shielding

Table 1
Eigenvalues of the fuel assemblies of BEAVRS at HZP.

	CASMO-4E	NECP-CACTI	Difference/pcm
16,000	0.98952	0.98944	-8
24,000	1.13130	1.13127	-3
24,012	1.00857	1.00837	-20
24,016	0.97033	0.97039	6
31,000	1.21279	1.21269	-10
31,006	1.15630	1.15614	-16
31,015	1.07251	1.07253	2
31,016	1.05786	1.05793	7
31,020	1.02229	1.02256	27

calculation, modular MOC method for the neutron-transport calculation, the TTA and CRAM methods for the depletion calculation. The 69-group microscopic cross-section libraries based on ENDF/B-VII.0 are generated and applied in NECP-CACTI for the lattice calculations.

According to the BEAVRS benchmark proposed by MIT (Horelik and Herman, 2013), there are 9 different kinds of fuel assemblies for the core simulations at HZP. With the same modeling and simulation parameters given by MIT, including the geometry, temperatures, isotope compositions and the configurations, the lattice calculations for the 9 different fuel assemblies are modeled and simulated by both NECP-CACTI and CASMO-4E. The eigenvalues of these fuel assemblies are compared as shown in Table 1.

In Table 1, 31,000, 31,006, 31,015, 31,016, 31,020, 24,000, 24,012, 24,016 and 16,000 represent the fuel assemblies 3.1% with 0 BA, 3.1% with 6 BA, 3.1% with 15 BA, 3.1% with 16 BA, 3.1% with 20 BA, 2.4% with 0 BA, 2.4% with 12 BA, 2.4% with 16 BA and 1.6% with 0 BA, where the percentage stands for the enrichment of ^{235}U and BA represents the burnable absorber. It can be observed that the differences in the eigenvalues of these fuel assemblies between NECP-CACTI and CASMO-4E are all within 30 pcm, which is small and acceptable. These comparisons assure that the modeling and simulations for the fuel assemblies of BEAVRS at HZP with the NECP-CACTI code are correct.

For the modeling and simulations of the radial baffle reflectors, ten different kinds of reflector assemblies are defined, with which the radial reflectors can be arranged and modeled for the core simulation. The ten kinds of reflector assemblies are defined as shown in Fig. 2. As an example shown in Fig. 3, the 1/8 corner of the radial reflector can be arranged and modeled by these reflector assemblies. With the similar arrangement and some essential rotations, these reflector assemblies can be used to model for the radial reflector of the full-core simulation. For these reflector assemblies defined for the radial baffle reflectors, NECP-CACTI is used to perform the 2D calculations to obtain the two-group constants of these radial baffle reflectors. Through the lattice calculations of the fuel assemblies and the radial baffle reflectors, the two-group constants can be obtained and provided to the steady-stated simulation of BEAVRS at HZP.

3.2. Core simulations with NECP-VIOLET

With the two-group constants provided by the lattice calculations using NECP-CACTI, the steady-state core simulation of BEAVRS at HZP is carried out by applying our home-developed neutron-diffusion solver NECP-VIOLET (Li et al., 2015b), which is

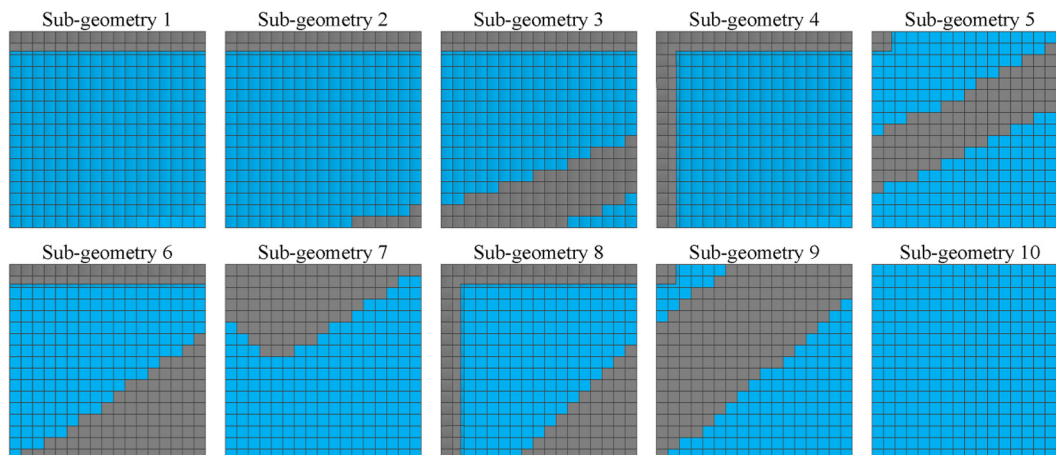


Fig. 2. Reflector assemblies defined for the radial baffle reflector.

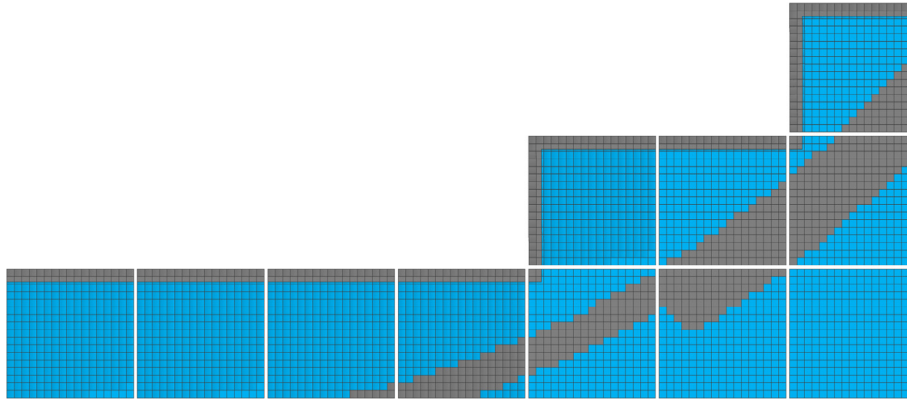


Fig. 3. Arrangement of the radial baffle reflector for core simulation.

based on the variational nodal method to solve the neutron-diffusion equation. To verify the core simulation, CASMO-4E was used in modeling and simulation of BEAVRS in 2D.

The multiplication factor of BEAVRS at HZP, predicted by NECP-CACTI and CASMO-4E are 0.99977 (−23 pcm) and 1.00031 (+31 pcm), respectively. The comparisons of the radial power distributions of BEAVRS at HZP are shown in Fig. 4. The RMS percent difference of the radial power distributions between NECP-VIOLET and CASMO-4E is 0.91%. For the “two-step” scheme of the core simulations, these differences are acceptable. Therefore, applying our home-developed lattice code NECP-CACTI and neutron-diffusion solver NECP-VIOLET, the correct modeling and simulations of BEAVRS at HZP can be implemented, which are the basis of the uncertainty analysis for BEAVRS at HZP in this paper.

4. Uncertainty analysis for BEAVRS at HZP

Based on the steady-state core modeling and simulation of BEAVRS at HZP using NECP-CACTI and NECP-VIOLET, the UNICORN code has been applied to perform the uncertainty analysis for BEAVRS at HZP according to the “two-step” scheme. For the lattice

0.709	0.801	0.804	0.971	0.872	0.966	0.939	1.004
0.699	0.789	0.796	0.960	0.868	0.965	0.948	1.019
-1.4	-1.5	-1.0	-1.1	-0.5	-0.1	1.0	1.5
0.801	0.767	0.938	0.868	1.007	0.900	1.133	1.065
0.789	0.758	0.924	0.862	0.998	0.902	1.135	1.065
-1.5	-1.2	-1.5	-0.7	-0.9	0.2	0.2	0.0
0.804	0.938	0.864	1.022	0.913	1.010	0.941	0.939
0.796	0.924	0.858	1.012	0.912	1.010	0.948	0.955
-1.0	-1.5	-0.7	-1.0	-0.1	0.0	0.7	1.7
0.971	0.868	1.022	0.951	1.095	1.024	1.187	0.779
0.960	0.862	1.012	0.951	1.096	1.031	1.187	0.776
-1.1	-0.7	-1.0	0.0	0.1	0.7	0.0	-0.4
0.872	1.007	0.913	1.095	1.444	1.193	1.269	
0.868	0.998	0.912	1.096	1.442	1.207	1.262	
-0.5	-0.9	-0.1	0.1	-0.1	1.2	-0.6	
0.966	0.900	1.010	1.024	1.193	1.250	0.936	
0.965	0.902	1.010	1.031	1.207	1.280	0.936	
-0.1	0.2	0.0	0.7	1.2	2.4	0.0	
0.939	1.133	0.941	1.187	1.269	0.936		
0.948	1.135	0.948	1.187	1.262	0.936		
1.0	0.2	0.7	0.0	-0.6	0.0		
1.004	1.065	0.939	0.779				CASMO4e
1.019	1.065	0.955	0.776				NECP-VIOLET
1.5	0.0	1.7	-0.4				Difference/%

Fig. 4. Comparisons of the radial power distributions between NECP-VIOLET and CASMO-4E.

Table 2

The isotopes and cross-section types analyzed in uncertainty analysis.

Cross section	Nuclides analyzed
$\sigma_{(n,elas)}$	$^{234}\text{U}, ^{235}\text{U}, ^{238}\text{U}, ^1\text{H}, ^{16}\text{O}, ^{90}\text{Zr}, ^{91}\text{Zr}, ^{92}\text{Zr}, ^{10}\text{B}, ^{11}\text{B}$
$\sigma_{(n,inel)}$	$^{234}\text{U}, ^{235}\text{U}, ^{238}\text{U}, ^{90}\text{Zr}, ^{91}\text{Zr}, ^{92}\text{Zr}, ^{10}\text{B}, ^{11}\text{B}$
$\sigma_{(n,2n)}$	$^{234}\text{U}, ^{235}\text{U}, ^{238}\text{U}, ^{90}\text{Zr}, ^{91}\text{Zr}, ^{92}\text{Zr}$
σ_f	$^{234}\text{U}, ^{235}\text{U}, ^{238}\text{U}$
σ_γ	$^{234}\text{U}, ^{235}\text{U}, ^{238}\text{U}, ^1\text{H}, ^{16}\text{O}, ^{90}\text{Zr}, ^{91}\text{Zr}, ^{92}\text{Zr}, ^{10}\text{B}, ^{11}\text{B}$
ν	$^{235}\text{U}, ^{238}\text{U}$
σ_α	$^{16}\text{O}, ^{10}\text{B}, ^{11}\text{B}$

calculations, the uncertainties of the multigroup microscopic cross sections are propagated to the eigenvalue and the two-group constants of the fuel assemblies; and for the steady-state core simulation, the uncertainties of the multiplication factor and the power distributions introduced by the uncertainties of the two-group constants are quantified.

4.1. Uncertainty analysis for the lattice calculations

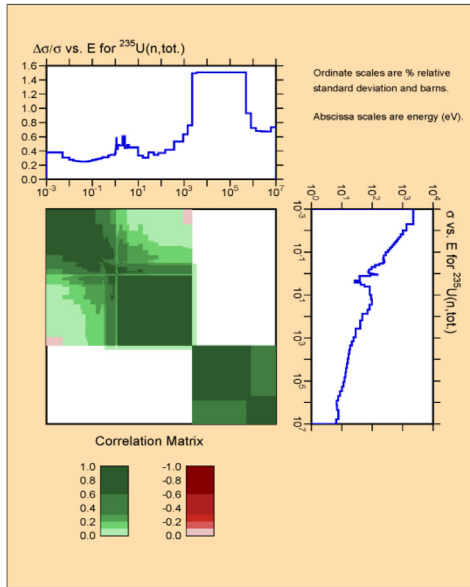
For the uncertainty analysis to the fuel assemblies of BEAVRS at HZP, the 69-group cross-section covariance libraries generated by ENDF/B-VII.1 are applied. Ten different re-samples with the sample size of 200 have been applied to the uncertainty analysis, with which the standard deviations of the relative uncertainties can be quantified. The main isotopes composed in the fuel assemblies analyzed in the uncertainty analysis are shown in Table 2.

The uncertainties of the isotopes and corresponding cross-section types listed in Table 2 have been propagated to the responses of the fuel assemblies of BEAVRS at HZP, and the relative uncertainty results are given in Table 3. The uncertainty results consist of two parts: the expectation values of the relative uncertainties and the standard deviation values of the relative uncertainties. The expectation values and standard deviation values of the relative uncertainties are calculated from the ten different re-samples by application of the bootstrap method.

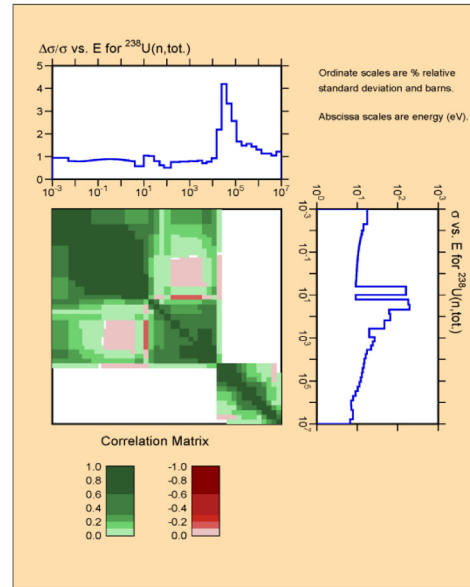
From the numerical results shown in Table 3, it can be observed that the relative uncertainties for the eigenvalues of the fuel assemblies vary from 0.50% to 0.57%; and the largest relative uncertainties of the two-group constants can up to be 1.65% for D_1 , the fast-group diffusion coefficient. Moreover, the relative uncertainties of the fast-group constants are larger than those of the thermal group. This is because that the nuclear-data uncertainties within the fast-group energy regions are much larger than those within the thermal-group energy regions. The relative uncertainties of the total cross sections for the isotopes ^{235}U , ^{238}U , ^1H and ^{16}O contained in ENDF/B-VII.1 are shown in Fig. 5.

Table 3
The relative uncertainties of the lattice-calculation responses for the fuel assemblies.

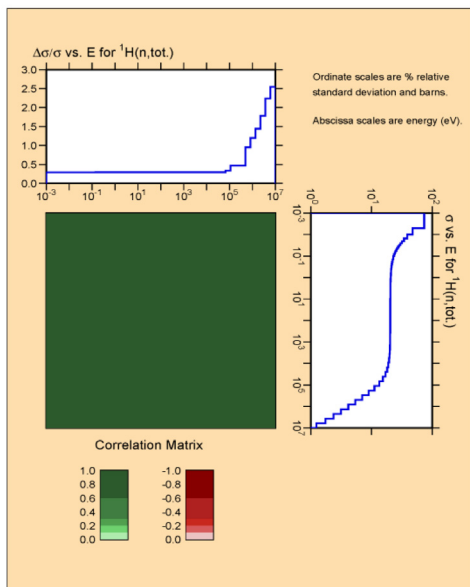
	16,000/%	24,000/%	24,012/%	24,016/%	31,000/%	31,006/%	31,015/%	31,016/%	31,020/%
k_{∞}	0.57 ± 0.02	0.52 ± 0.02	0.52 ± 0.02	0.52 ± 0.02	0.50 ± 0.02				
D_1	1.65 ± 0.11	1.62 ± 0.11	1.64 ± 0.11	1.65 ± 0.11	1.60 ± 0.11	1.61 ± 0.11	1.62 ± 0.11	1.63 ± 0.11	1.63 ± 0.11
D_2	0.37 ± 0.02								
$\Sigma_{a,1}$	1.02 ± 0.06	0.96 ± 0.05	0.96 ± 0.05	0.96 ± 0.05	0.92 ± 0.05	0.92 ± 0.05	0.92 ± 0.05	0.93 ± 0.05	0.93 ± 0.05
$\Sigma_{a,2}$	0.44 ± 0.02	0.39 ± 0.01	0.34 ± 0.01	0.33 ± 0.01	0.36 ± 0.01	0.34 ± 0.01	0.32 ± 0.01	0.31 ± 0.01	0.30 ± 0.01
$\nu\Sigma_{f,1}$	1.03 ± 0.05	0.76 ± 0.04	0.76 ± 0.04	0.75 ± 0.04	0.64 ± 0.03	0.63 ± 0.03	0.63 ± 0.03	0.63 ± 0.03	0.62 ± 0.03
$\nu\Sigma_{f,2}$	0.39 ± 0.01	0.38 ± 0.01							
$\Sigma_{s,1,1}$	1.01 ± 0.06	1.01 ± 0.06	1.01 ± 0.06	1.02 ± 0.06	1.00 ± 0.06	1.00 ± 0.06	1.01 ± 0.06	1.01 ± 0.06	1.01 ± 0.06
$\Sigma_{s,1,2}$	1.18 ± 0.06	1.11 ± 0.06	1.18 ± 0.06	1.21 ± 0.06	1.08 ± 0.06	1.11 ± 0.06	1.16 ± 0.06	1.16 ± 0.06	1.18 ± 0.06
$\Sigma_{s,2,1}$	0.57 ± 0.03	0.55 ± 0.03	0.53 ± 0.03	0.53 ± 0.03	0.54 ± 0.03	0.54 ± 0.03	0.52 ± 0.03	0.52 ± 0.03	0.52 ± 0.03
$\Sigma_{s,2,2}$	0.35 ± 0.02	0.35 ± 0.02	0.36 ± 0.02	0.36 ± 0.02	0.35 ± 0.02	0.36 ± 0.02	0.36 ± 0.02	0.36 ± 0.02	0.36 ± 0.02



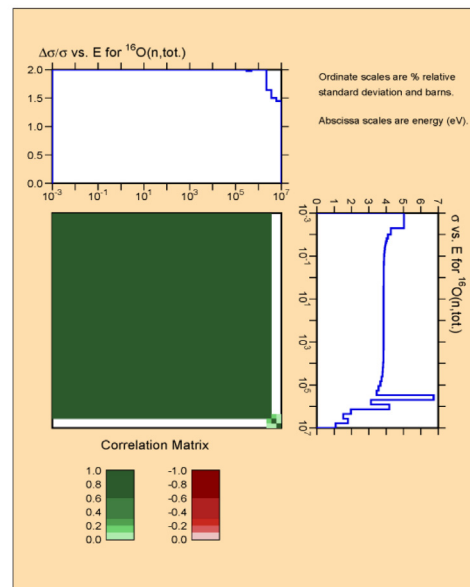
(a). Relative uncertainty of $^{235}\text{U}-\sigma_t$



(b). Relative uncertainty of $^{238}\text{U}-\sigma_t$



(c). Relative uncertainty of $^1\text{H}-\sigma_t$



(d). Relative uncertainty of $^{16}\text{O}-\sigma_t$

Fig. 5. The relative uncertainties of total cross sections for ^{235}U , ^{238}U , ^1H and ^{16}O .

4.2. Uncertainty analysis for the core simulation

As the samples and relative covariance matrices of the two-group constants can be obtained by the uncertainty analysis for the lattice calculations using the SS method, two sampling methods are applied to the uncertainty analysis for the core simulation of BEAVRS at HZP. For the sampling method based on the covariance matrices of the two-group constants, ten different re-samples with the sample size of 200 have been applied. For the sampling method based on the samples of the two-group constants, all the 2000 samples obtained by the uncertainty analysis of the lattice calculations are utilized. The relative uncertainties of the multiplication factor and power distributions are quantified by applying these two kinds of sampling methods, with the “Mac_Sample” standing for the sampling method using the samples of the two-group constants and “Cov_Sample” representing the sampling method using the relative covariance matrices of the two-group constants.

For the uncertainty analysis of the core simulation of BEAVRS at HZP, both the 2D and 3D simulations are applied. With the 2D core simulation, Table 4 shows the relative uncertainties of the multiplication factor, and the radial power distributions and relative uncertainties are presented in Fig. 6. With the 3D core simulation, Table 5 shows the relative uncertainties of the multiplication factor, and the relative uncertainties of the axial and radial power distributions are presented in Fig. 7.

From the uncertainty results for the 2D core simulation, it can be observed that the relative uncertainty in the multiplication factor of the core simulation is about 5.1% as shown in Table 4, which is of the same magnitude as the uncertainties encountered in the eigenvalues of the fuel assemblies. As shown in Fig. 6, it can be observed that the maximum relative uncertainty of the 2D radial power distributions is 4.27%, occurred in the middle of the reactor

Table 4
The relative uncertainties in k_{eff} of the 2D core simulation for BEAVRS at HZP.

Conditions	k_{eff}	Methods	$\Delta k_{eff}/k_{eff}\%$
2D	0.99977	Mac_Sample	0.51
		Cov_Sample	0.51 ± 0.019

0.70	0.79	0.80	0.96	0.87	0.97	0.95	1.02
4.27	3.98	3.47	2.68	1.91	0.70	0.66	1.69
3.99±0.20	3.71±0.18	3.24±0.16	2.50±0.12	1.78±0.09	0.66±0.03	0.62±0.03	1.56±0.08
0.79	0.76	0.92	0.86	1.00	0.90	1.14	1.07
3.98	3.82	3.21	2.60	1.66	0.62	0.89	1.79
3.71±0.18	3.56±0.18	2.99±0.15	2.42±0.12	1.55±0.08	0.59±0.03	0.83±0.04	1.66±0.08
0.80	0.92	0.86	1.01	0.91	1.01	0.95	0.96
3.47	3.21	2.80	2.02	1.27	0.16	0.99	1.87
3.24±0.16	2.99±0.15	2.61±0.13	1.88±0.09	1.18±0.06	0.15±0.01	0.92±0.05	1.73±0.09
0.96	0.86	1.01	0.95	1.10	1.03	1.19	0.78
2.68	2.60	2.02	1.30	0.28	0.59	1.63	1.93
2.50±0.12	2.42±0.12	1.88±0.09	1.21±0.06	0.25±0.01	0.56±0.03	1.52±0.07	1.77±0.09
0.87	1.00	0.91	1.10	1.44	1.21	1.26	
1.91	1.66	1.27	0.28	0.83	1.55	2.23	
1.78±0.09	1.55±0.08	1.18±0.06	0.25±0.01	0.79±0.04	1.46±0.07	2.08±0.10	
0.97	0.90	1.01	1.03	1.21	1.28	0.94	
0.70	0.62	0.16	0.59	1.55	2.28	2.52	
0.66±0.03	0.59±0.03	0.15±0.01	0.56±0.03	1.46±0.07	2.14±0.11	2.34±0.12	
0.95	1.14	0.95	1.19	1.26	0.94		
0.66	0.89	0.99	1.63	2.23	2.52		
0.62±0.03	0.83±0.04	0.92±0.05	1.52±0.07	2.08±0.10	2.34±0.12		
1.02	1.07	0.96	0.78				Power
1.69	1.79	1.87	1.93				Mac_Sample/%
1.56±0.08	1.66±0.08	1.73±0.09	1.77±0.09				Cov_Sample/%

Fig. 6. The radial power distributions and relative uncertainties of BEAVRS at HZP.

Table 5
The relative uncertainties in k_{eff} of the 3D core simulation for BEAVRS at HZP.

Conditions	k_{eff}	Methods	$\Delta k_{eff}/k_{eff}\%$
3D	0.99610	Mac_Sample	0.53
		Cov_Sample	0.53 ± 0.021

with lower assembly power. The RMS of the relative uncertainties of the 2D radial power distributions is 2.08%.

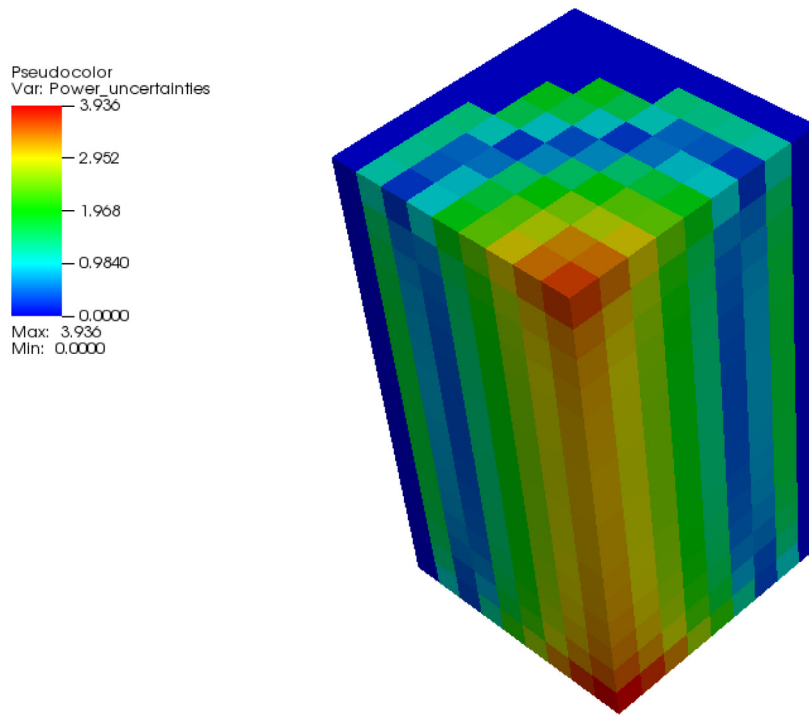
From the uncertainty results for the 3D core simulation, it can be observed that the relative uncertainty in the multiplication factor of the core simulation is about 5.3% as shown in Table 5, which is also of the same magnitude as the uncertainties encountered in the eigenvalues of the fuel assemblies. As shown in Fig. 7(a), the largest relative uncertainty of the 3D power distributions is 3.94%, occurred in the middle assembly of the bottom layer. From Fig. 7 (b), it can be observed that the relative uncertainties existed in the axial power distributions are far less than those in the radial power distributions, with the largest relative uncertainty of 0.81%. This phenomenon is reasonable, as the axial power distributions are the integral variables based on the radial power distributions. From the results of Fig. 7(b), the implied conclusion can be given that the relative uncertainties existed in the AO values will be not notable.

In order to find out the most significant uncertainty sources to the response uncertainties of the core simulations, detailed analysis towards the uncertainty contributions of every single fuel assembly and corresponding few-group constants has been performed to the multiplication factor based on the 3D modeling. In this analysis, the covariance matrices of the few-group constants between different fuel assemblies are neglected for the purpose of quantifying the uncertainty contributions of every single fuel assembly. The uncertainty contributions of every single fuel assembly and corresponding few-group constants to the uncertainty of the multiplication factor are shown in Table 6.

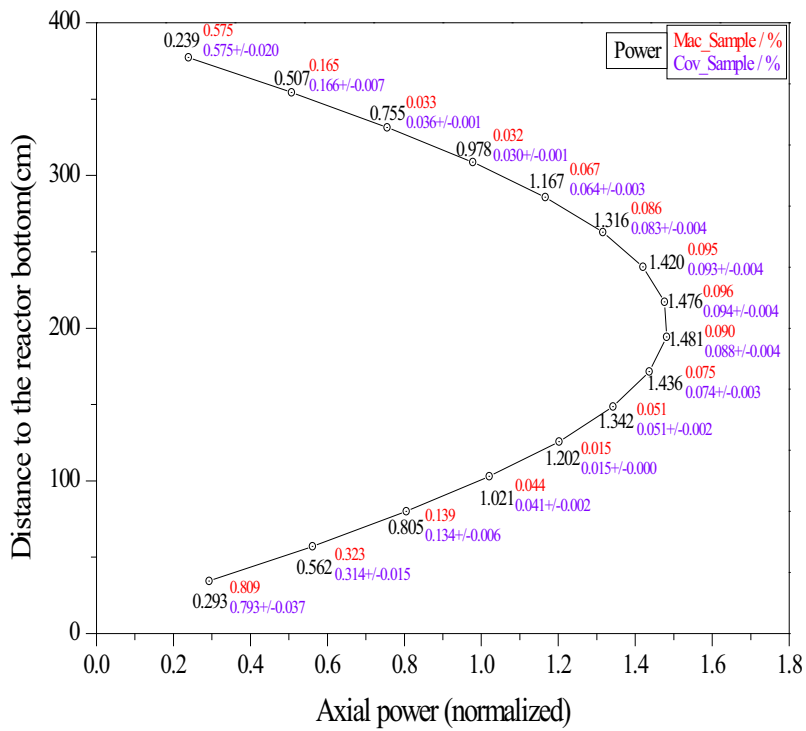
From the numerical results shown in Table 6, two aspects of observations can be obtained. Firstly, the covariance matrices of the few-group constants between different fuel assemblies have significant contributions to the uncertainty results of the core simulations, as the summation of the relative uncertainties caused by every single fuel assembly is only 1.97%, far less than the results 0.53% as shown in Table 5. Therefore, the covariance matrices of the few-group constants between different fuel assemblies should be taken into account for the uncertainty analysis of the core simulations. Secondly, from the analysis towards uncertainty contributions of every kind of few-group constants, it can be found that the most significant constants to the uncertainty results is $\nu\Sigma_f$, not the diffusion constants, which have the largest uncertainties in the lattice calculations as shown in Table 3.

For the uncertainty results with Mac_Sample and Cov_Sample, it can be observed that the discrepancy exists between these two methods. The Mac_Sample method is recommended for the uncertainty analysis of core simulations, as the Cov_Sample method will introduce statistical errors or un-consistency to the few-group constants by re-sampling with the covariance matrices. Therefore, the Mac_Sample method will be preferred for the uncertainty analysis of the core simulations, especially for the cycle calculations.

From the view of the reactor-physics simulations, these uncertainties are notable for the fresh core at HZP, and they are expected higher for the depleted core at HFP. Therefore, these uncertainties should be taken into account for the safety analysis and economic competitiveness of the reactor system.



(a). Relative uncertainties of the 3D power distributions / %



(b). Relative uncertainties of the axial power distributions / %

Fig. 7. The relative uncertainties of power distributions with 3D simulation of BEAVRS at HZP.

Table 6

The uncertainty contributions of every single fuel assembly and corresponding few-group constants.

	$D/\%$	$v\Sigma_f/\%$	$\Sigma_s/\%$	$Adff/\%$	Total/%
16,000	1.22E-02	1.08E-01	3.60E-02	1.15E-03	1.14E-01
24,000	2.14E-03	2.25E-02	7.26E-03	4.47E-04	2.38E-02
24,012	5.82E-03	7.25E-02	1.64E-02	1.10E-03	7.46E-02
24,016	1.08E-02	1.03E-01	2.18E-02	1.74E-03	1.06E-01
31,000	3.21E-02	5.60E-02	3.89E-02	8.61E-04	7.54E-02
31,006	6.82E-03	2.67E-02	1.23E-02	1.50E-03	3.02E-02
31,015	9.57E-04	1.68E-02	6.13E-03	7.37E-04	1.79E-02
31,016	6.13E-04	2.80E-02	9.66E-03	9.72E-04	2.96E-02
31,020	1.63E-03	2.53E-02	7.06E-03	6.83E-04	2.63E-02
Sum	3.72E-02	1.83E-01	6.28E-02	3.27E-03	1.97E-01

5. Conclusions

In this paper, the uncertainty-analysis capability for the reactor-physics simulations based on the “two-step” scheme has been implemented in our home-developed UNICORN code. The nuclear-data uncertainties are firstly propagated to the uncertainties of the assembly few-group constants of the lattice calculations, and then the uncertainties of the assembly few-group constants are propagated to the uncertainties of the multiplication factor and power distributions of the steady-state core simulations. The statistical sampling method is applied to the uncertainty analysis for both the lattice and core simulations with our home-developed lattice code NECP-CACTI and neutron-diffusion solver NECP-VIOLET respectively.

With NECP-CACTI and NECP-VIOLET, the modeling and simulation of the steady-state BEAVRS benchmark problem at HZP was performed and the corresponding results were compared against those obtained with CASMO-4E. The verification proves that modeling and simulation of BEAVRS at HZP with NECP-CACTI and NECP-VIOLET are correct.

Based on the correct modeling and simulation, the UNICORN code was then applied to perform uncertainty analysis to BEAVRS at HZP according to the “two-step” scheme. From the uncertainty results of the lattice calculations, it can be observed that the relative uncertainties for the eigenvalues of the fuel assemblies vary from 0.5% to 0.57% for different assemblies; and the largest relative uncertainties of the two-group constants can up to be 1.65% for D_1 . From the uncertainty analysis of the core simulation of BEAVRS at HZP, it can be observed that for the multiplication factor, the relative uncertainty is about 5.1‰ for the 2D core simulation and 5.3‰ for the 3D core simulation, which is of the same magnitude as the uncertainties encountered in the eigenvalues of the fuel assemblies. For the radial power distributions, the largest uncertainty occurred in the middle of the core with a maximum value of 4.27% and the RMS value of 2.08%; while for the axial power distributions, the largest relative uncertainty exist in the bottom layer with value of 0.81%. With detailed analysis of the uncertainty contributions for every single fuel assemblies and corresponding few-group constants, it can be observed that the covariance matrices of the few-group constants between different fuel assemblies play significant contributions to the uncertainty results of the core simulation, hence should be taken into account in the uncertainty analysis for the core simulations.

Through the nuclear-data uncertainty propagations from the lattice calculations to the steady-state core simulations, it can be found that the uncertainties exist in the multiplication factor and power distributions of the core simulations are notable and should be taken into account for the reactor-physics simulations, hence for the safety analysis and economic competitiveness of the reactor system.

Acknowledgements

This work is supported by the National Natural Science Foundation of China (Grant No. 11522544).

References

- Archer, G.E.B., Saltelli, A., Sobol, I.M., 1997. Sensitivity measures, anova-like techniques and the use of bootstrap. *J. Stat. Comput. Simul.* 58, 99–120.
- Ball, M.R., Novog, D.R., Luxat, J.C., 2013. Analysis of implicit and explicit lattice sensitivity using DRAGON. *Nucl. Eng. Des.* 265, 1–12.
- Foad, B., Takeda, T., 2015. Sensitivity and uncertainty analysis for UO₂ and MOX fueled PWR cells. *Ann. Nucl. Energy* 75, 595–604.
- Horelik, N., Herman, B., 2013. Benchmark for Evaluation And Validation of Reactor Simulations rev. 1.1.1. MIT Computational Reactor Group.
- Ivanov, K., Avramova, M., Kamerow, S., Kodeli, I., Sartori, E., Ivanov, E., Cabellos, O., 2013. Benchmarks for Uncertainty Analysis in Modelling (UAM) for the Design, Operation and Safety Analysis of LWRs. OECD Nuclear Energy Agency, NEA/NSC/DOC(2013) 7.
- Leszczynski F., Aldama D. L., Trkov A., 2007. WIMS-D Library Update: Final Report of a Coordinated Research Project. International Atomic Energy Agency.
- Li, Y., Tian, C., Zheng, Y., et al., 2015a. NECP-CACTI: Pressurized Water Reactor Lattice Code Development, Transactions of the American Nuclear Society, vol. 112, San Antonio.
- Li, Y., Wang, Y., Liang, B., Shen, W., 2015b. Partitioned-Matrix acceleration to the Fission-Source iteration of the Variational Nodal Method. *Prog. Nucl. Energy* 85, 640–647.
- Marleau G., Hébert A., Roy R., 2014. A User Guide for DRAGON Version 5. Technical Report, IGE-335.
- Pusa, M., 2012. Incorporating sensitivity and uncertainty analysis to a lattice physics code with application to CASMO-4. *Ann. Nucl. Energy* 40, 153–162.
- Rhodes, J., Smith, K., Edenius, M., 2004. CASMO-4E: Extended Capability CASMO-4, User's Manual. Studsvik Scandpower, Report SSP-09/443 University Release.
- Wan, C., Cao, L., Wu, H., et al., 2015. Code development for eigenvalue total sensitivity analysis and total uncertainty analysis. *Ann. Nucl. Energy* 85, 788–797.
- Wieselquist W., Zhu T., Vasiliev A., et al., 2012. PSI Methodologies for Nuclear Data Uncertainty Propagation with CASMO-5M and MCNPX: Results for OECD/NEA UAM Benchmark Phase I. Science and Technology of Nuclear Installations, vol. 2013, Article ID 549793. doi: 10.1155/2013/549793.
- Yankov A., Klein M., Jessee M. A., Zwermann W., Velkov K., Pautz A., Collins B., Downar T., 2012. Comparison of XSUSA and “Two-step” Approaches for Full-core Uncertainty Quantification. *PHYSOR 2012*, Tennessee, USA.
- Zu, T., Wan, C., Cao, L., et al., 2016. Total uncertainty analysis for PWR assembly based on the statistical sampling method. *Nucl. Sci. Eng.* 183, 371–386.